

Ferrocenoyl Phenylalanine: A New Strategy Toward Supramolecular Hydrogels with Multistimuli Responsive Properties

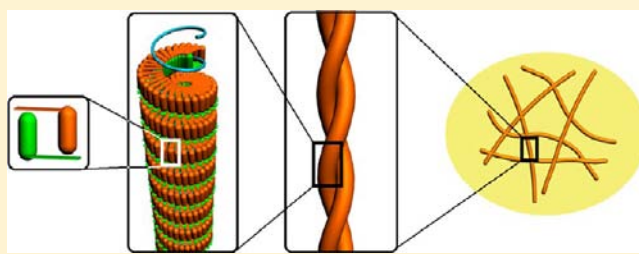
Zhifang Sun,^{†,||} Zhengyuan Li,^{†,||} Yonghui He,[§] Rujuan Shen,[‡] Liu Deng,[†] Minghui Yang,[†] Yizeng Liang,[†] and Yi Zhang^{†,*}

[†]Key Laboratory of Resources Chemistry of Nonferrous Metals (Ministry of Education), College of Chemistry and Chemical Engineering and [‡]State Key Laboratory of Powder Metallurgy, Central South University, Changsha 410083, China

[§]Key Laboratory of Chemistry in Ethnic Medicinal Resources, Yunnan University of Nationalities, Kunming 650500, China

S Supporting Information

ABSTRACT: In this paper we present a new paradigm for designing hydrogelators that exhibit sharp phase transitions in response to a series of disparate stimuli, including oxidation–reduction reactions (redox), guest–host interactions, and pH changes. We have serendipitously discovered that ferrocenoyl phenylalanine (Fc-F) monomers aggregate in water via a rapid self-assembly mechanism to form stable, multistimuli hydrogels. In comparison to other known mono- and multi-responsive gelators, Fc-F is unique because of its small size, economy of gel-forming components, and exceptionally simple molecular structure. Density functional theory (DFT) *ab initio* calculations suggest gel formation initially involves an antiparallel, noncovalent dimerization step wherein the ferrocenoyl moiety of one axe-like monomer conjoins with the phenyl group of the second monomer via a π – π stacking interaction to form brick-like dimers. This stacking creates a cavity in which the carboxylic acid groups of each monomer mutually interact via hydrogen bond formation, which affords additional stability to the dimer. On the basis of structural analysis via optical and electrical measurements and additional DFT calculations, we propose a possible stepwise hierarchical assembly mechanism for fibril formation. Insights into the self-assembly pathway of Fc-F should prove useful for understanding gelation processes of more complex systems. We expect that Fc-F will serve as a helpful archetypical template for others to use when designing new, stimuli specific hydrogelation agents.



■ INTRODUCTION

Stimuli responsive supramolecular gelling agents have been the focus of considerable recent research,¹ owing, in part, to their proposed use as components in molecular motors,² signal sensors,³ shape memories,⁴ drug deliverers,⁵ display devices,⁶ and other applications.⁷ Low molecular weight gelators (LMWG, <500 amu) that undergo reversible gel–sol transformations in response to a variety of disparate stimuli, such as redox reagents, pH changes, or chelation, have been of particular interest because of their potential ability to act as multi-input logic gates.⁸ Supramolecular gelators typically are made up of a variety of covalently linked functional groups that foster the growth of noncovalently linked oligomers via a self-assembly process.⁹ Despite the availability of a growing number of well characterized LMWG gelators,^{10,11} theoretical and practical chemists continue to find it difficult, if not impossible, to a priori predict whether or not materials will be a gelator. This difficulty stems from, and attests to, the complex, 3D intermolecular nature of gels.¹² As a consequence, the current catalogs of known mono- and multiresponsive gelators are available because of serendipitous discoveries or modifications to the molecular structure of such materials. The development of a rational approach for designing simple but effective gelators

having sharp, rapidly reversible, functional responsive abilities to one or more stimuli remains a formidable challenge.¹³

In this report we describe our serendipitous discovery of an exceptionally simple hydrogelator, ferrocenoyl phenylalanine (Fc-F), and present the preliminary results of our efforts to understand the effect that molecular structure has on its gel forming ability. While our design and synthesis of Fc-F owes much to the innovative efforts of a number of research groups,^{14,15} two pioneering research reports were particularly inspirational for our work. The first report described an organogelator that was composed of a ferrocenoyl moiety that attached to a cholesterol group via a short peptide linkage.¹⁶ From our point of view this use of ferrocene as an aromatic π – π bonding agent was intriguing for several reasons. First, ferrocene is chemically stable and has relatively low acute toxicity.¹⁷ Second, it is electrochemically active and has been used as a mediator in electrochemical redox reactions of enzymes.¹⁸ Moreover, because of our strong interest in developing a multiresponsive gelator, this finding that treatment of the Fc-containing gel with Ce⁴⁺ ions caused the gel to

Received: April 4, 2013

Revised: August 8, 2013

Published: August 11, 2013

collapse into a liquid phase suggests that oxidants found in vivo, such as H_2O_2 , might cause similar behavior in gels wherein the ferrocene moiety plays an important role in the gelation process. The second report that provided guidance to our effort described an important discovery that 9-fluorenylmethoxycarbonyl diphenylalanine (Fmoc-FF), although of relative small size as compared to most gelators, nonetheless was an organogelator.¹⁹ Although this study stressed the important role that a fluorenyl aromatic group could contribute to gelation via the formation of intermolecular π - π stacking interactions, we were particularly interested in the potential ability of the F moiety to participate in intermolecular coupling with its neighbors via both hydrogen bonding and π - π stacking interactions. With these two studies in mind, we synthesized Fc-FF as a potential redox responsive organogelator, which indeed proved to be the case. More important, however, was our discovery that a precursor to this material, namely Fc-F, underwent a gelation reaction when dispersed in water. Remarkably, the deletion of a single F group converts an organogelator into a hydrogelator. To the best of our knowledge, Fc-F is the smallest, most structurally simple multistimuli responsive hydrogelator that has ever been discovered.

The small size and extreme structural simplicity of Fc-F are appealing for a number of reasons. First, monomers having minimal atomic makeup have the possibility of being studied individually and in combination with intermolecular neighbors using *ab initio* density functional theory (DFT) calculations. The results of such calculations could provide insights into the stepwise self-assembly pathway that this and, by extension, other gelators take when forming supramolecular oligomers. Second, monomers having relatively simple molecular structures hold the promise of synthetic ease and low cost. Third, the tenets of green chemistry dictate that targeted molecules should be composed of environmentally friendly components while concomitantly having the best atomic economy possible (minimized atom count).

RESULTS

Gelation Properties of Fc-F. Morphological Study.

Figure 1A shows the molecular structure of Fc-F. Our experiments suggest that in water the critical gelation concentration (weight/weight) of Fc-F is between 0.2 and 0.3 wt % (2–3 $mg \cdot mL^{-1}$) at room temperature (Supporting Information (SI) Figure S1). We used a variety of microscopy techniques to obtain local structural information of Fc-F

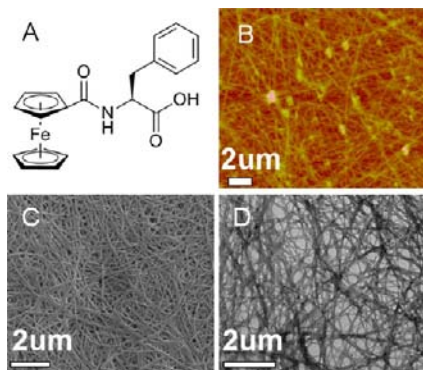


Figure 1. (A) Chemical structure of the gelator Fc-F. (B–D) AFM, SEM, and TEM images of the cryo-dried hydrogel, respectively.

hydrogels. Hydrogel sample preparation involved freezing samples in a liquid nitrogen bath followed by a vacuum freeze-drying step (cryo-drying).

Images obtained using atomic force microscopy (AFM images, Figure 1B), scanning electron microscopy (SEM, Figure 1C), and transmission electron microscopy (TEM, Figure 1D) confirm that the scaffolds of the Fc-F hydrogel are well-organized fibrils having widths of 30–80 nm and lengths reaching ≥ 1 μm . It needs to be highlighted that Fc-F is a rare example of ferrocene derived peptides that aggregate to homogeneous fibrils.

Fc-F hydrogels are very stable and retain their original gel state for at least nine months when stored at $pH \cong 7.0$; under mildly acidic conditions ($pH < 6.0$) crystal growth was observed to occur within the gel approximately six weeks after gel formation (SI Figures S2 and S3). Fc-F gelator is readily synthesized and easily purified in high yield (90%) (Supporting Information).

In order to evaluate the role that phenylalanine plays in the gelation process, we also synthesized the following series of Fc-amino acid conjugates: Fc-Tyrosine, Fc-Tryptophan, Fc-Histidine, Fc-Alanine, and Fc-Lysine. None of these compounds were observed to form hydrogels, which therefore suggests that the phenyl group of Fc-F plays a critically important role in gel formation.

Rheological Study. To verify the viscoelastic properties of Fc-F gels, we performed dynamic frequency sweep and dynamic time sweep measurements on the gel. As shown in Figure 2A, the values of the storage modulus (G') were about

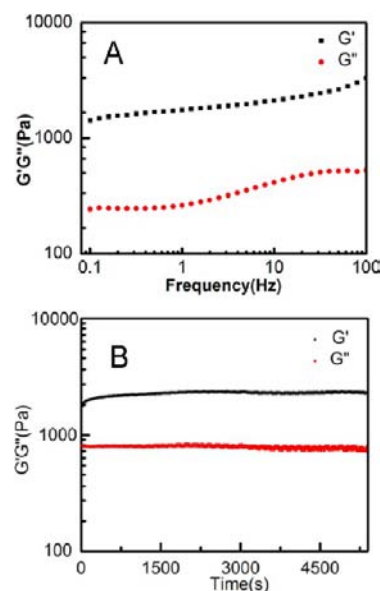


Figure 2. (A) Dynamic frequency sweep of the storage moduli, G' , and the loss moduli, G'' , of the hydrogel, measured at 2% strain. (B) Dynamic time sweep of G' and G'' of the hydrogel at the strain of 0.3% and at the frequency of 1 rad/s. All measurements were performed at 298 K and at a concentration of 5 $mg \cdot mL^{-1}$ hydrogel.

six times that of the loss modulus (G'' in the scanning range studied, indicating that the sample is a true hydrogel. The G' values increased with increasing frequency. The G'' curve had a flattened S shape which contained two flat regions in the frequency ranges of 0.1–1 Hz and 500–100 Hz, respectively.

The G' value of the Fc-F hydrogel was about 1800 at 1 rad/s, indicating that it has both liquid and solid characteristics.²⁰ Dynamic time sweep data shows that the value of G' increased slightly in the first 10 min after gel formation but then was essentially constant for the remaining incubation period (Figure 2B). The value of G'' remained constant during the entire measurement. From those rheological findings we conclude that Fc-F hydrogels are medium-strength physical gels.

Responsive Properties of Fc-F Hydrogel. *Responsivity to pH Changes.* The operational pH range for Fc-F hydrogel formation is pH 5–8 at room temperature. Below pH 5, the gel phase undergoes a transformation that results in the formation of a precipitate. TEM images show that the scaffolds of these precipitates consist of short fibrils (SI Figure S4). Above pH 8, Fc-F exists in its liquid state (Figure 3). Microscopic analysis of cryo-dried samples of this material shows that Fc-F has lost its network structure although short ribbon-like fragments can be discerned (SI Figure S5).



Figure 3. Reversible gel–sol transitions of the supramolecular hydrogel triggered by multiple stimuli (pH, chemical redox reaction, shear stress, and temperature, respectively).

Responsivity to Chemical Redox. Ferrocene can be chemically or electrochemically oxidized to ferrocinium cation with loss of its aromaticity. Fang and co-workers reported that a group of organogels containing Fc moieties underwent a gel to sol transition when treated with Ce^{4+} oxidants.¹⁶ They suggested that the oxidation of Fc was responsible for this behavior. Because hydrogen peroxide is ubiquitous in living systems, we investigated its effects on gel stability. Although the oxidation potential of H_2O_2 is less than that of Ce^{4+} , we nonetheless found that treatment of Fc-F gel with a 30% solution of this oxidant also initiated a gel to liquid transition and thus provides a rare example of a hydrogel that responds to H_2O_2 . The importance of this observation is 2-fold. First, it supports the importance of ferrocene's role in aromatic mediated intermolecular π – π stacking in dimer formation. Second, it suggests that H_2O_2 might be able to be exploited as a switch to control the release of drugs embedded in Fc-F hydrogels.

Several additional experiments were performed to verify the importance of the Fc moiety in forming hydrogels. In the first experiment, 50 μ L of H_2O_2 solution (30%) was carefully added to the top of a preformed hydrogel surface. The hydrogel slowly began to liquefy, with the concomitant formation of a light green suspension (Figure 3). SI Figure S6a shows a typical SEM image of a cryo-dried Fc-F gel obtained from the surface of an Fc-F gel 10 min after being treated in this manner. This oxidation-induced gel to sol transformation was complete in

several hours at room temperature. We noted that mixtures of ferrocinium ions and peptide aggregates were amorphous powders (SI Figure S6b).

When proper amounts of ascorbic acid basic solution were injected into samples of H_2O_2 induced liquefied Fc-F, a yellow sol appeared shortly when the solution was shaken and a sol to gel phase transition occurred after the pH value was adjusted back to 6–8. The significant difference between the oxidation and reduction reaction rates suggests that the penetration of H_2O_2 into the inner zone of the Fc-F scaffolds was significantly slower than the penetration of ascorbic acid into the aqueous solution of amorphous aggregates.

Responsivity to Electrochemical Redox. Cyclic voltammetry experiments indicated that the $E^{\circ}_{1/2}$ of Fc-F was approximately 0.4 V (vs Ag/AgCl), close to the $E^{\circ}_{1/2}$ potential reported for ferrocene²¹ (SI Figure S7). We therefore performed potentiostatic electrolysis experiments on Fc-F hydrogels at 0.6 V and 0.2 V (vs Ag/AgCl) to determine the electrochemical redox-driven phase-transition behavior of Fc-F. By carefully designing the electrode area and hydrogel film thickness, we were able to demonstrate switching between gel and sol phases as a function of redox potential.

Ligand–Receptor Responsivity. It is well-known that ferrocene can enter the internal hydrophobic cavity of β -cyclodextrin and establish a strong guest–host interaction. We have found that this strong guest–host association can overwhelm intermolecular interactions between Fc-F molecules and inhibit gelation. This is demonstrated by the failure of Fc-F monomer to form a hydrogel in the presence of β -cyclodextrin: We stoichiometrically premixed β -cyclodextrin and Fc-F (1:1) in DMSO solution and then added the mixed solution into a phosphate buffer, the mixture presented as a clear solution, and we were not able to form the gel yet, even by increasing the concentration of Fc-F to 12 $mg \cdot mL^{-1}$ (5-fold to the critical gelation concentration of Fc-F). The electronic microscopy images (SI Figure S8) confirmed that the mixture of β -cyclodextrin and Fc-F monomer was not able to assemble to fibrils.

Gently adding β -cyclodextrin into a pre-existing Fc-F hydrogel caused a slow and small change to the hydrogel at room temperature, suggesting the disassembly process of the Fc-F assemblies is still a thermodynamically favored but dynamically disfavored process in the presence of β -cyclodextrin in the gel.

When a mixture of β -cyclodextrin and Fc-F hydrogel was heated to 338 K, the hydrogel state degraded to the sol phase and the gel phase did not reappear after reaction conditions returned to room temperature, confirming that the driving forces for Fc-F dimerization are mainly physical interactions; each of them is weaker than the interaction between Fc moieties and β -cyclodextrin.

Other Properties with Application Potentiality. *Electron Transfer Matrix for Immobilized Enzymes.* In a previous work we demonstrated that Fc-FF nanowires could serve as a novel probe for the detection of the tumor necrosis factor- α in bulk solution.²² Our current investigation has shown that Fc-F hydrogels not only can provide an aqueous environment for enzyme immobilization but also serve as an electron transfer mediator for enzyme electron transfer due to the facile electron transfer of Fc.

Figure 4A shows the CVs of the Fc-F gel coated electrode in the buffer solution and the glucose oxidase (GOD) immobilized gel coated electrode, respectively. The red curve

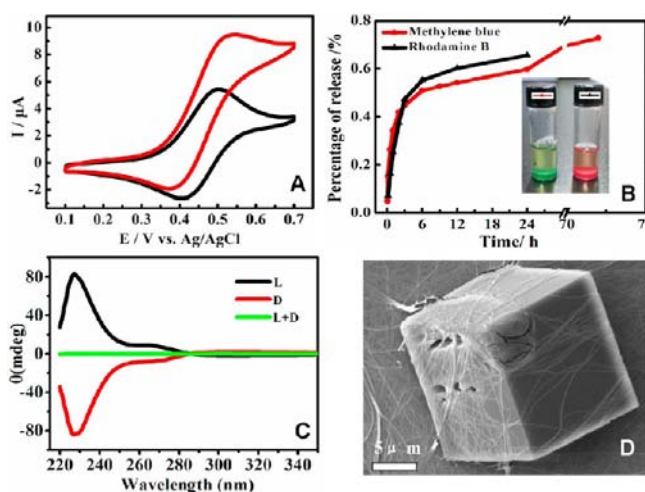


Figure 4. (A) Cyclic voltammetry curves of the GOD/Fc-F hydrogel with (PBS, pH = 7.4, red curve) and without glucose (black). (B) Drug release curves of the Fc-F hydrogel. (C) CD signals for *d*-, *l*-, and racemic Fc-F, respectively. (D) SEM image of the cryo-dried hydrogel in saturated NaCl solution.

represents a typical electrocatalytic oxidative curve of glucose with a sharp increase of oxidation current and a decreased reduction current, suggesting that indeed the oxidation of glucose is catalyzed by GOD, which is in turn mediated by Fc. This demonstrates the utility of the hydrogel in the mobilization of fragile enzymes.

Drug Immobilizations and Controlled Releases. Phenylalanine is a naturally occurring amino acid and therefore is innocuous in biological systems; ferrocene has relatively low acute toxicity according to data available in MSDS documents. We have not yet conducted toxicity studies of Fc-F, since both the Fc and the F groups can be considered to be relatively biologically friendly. Fc-F gels have the potential to function as drug delivery carriers. For drug delivery purposes, the drug must be loaded into the gel, which requires that the drug does not disturb the gelation. Considering that the incorporation of aromatic molecules might inhibit or degrade Fc-F gel states, we added two aromatic dyes, rhodamine B and methylene blue, to Fc-F gels, respectively. We were pleased to find that the presence of neither dye had a significant effect on the gel phase of Fc-F. Kinetic-release curves for both dyes from Fc-F hydrogels to a surrounding water phase are shown in Figure 4B, suggesting that the gel has pores that are large enough to allow incorporated materials to escape, thereby demonstrating it has the potential to be used as a generic drug releasing medium.

Chiral Features. Another key feature of the hydrogel is that, depending on the enantiomeric nature of the phenylalanine used in the synthesis of Fc-F, it can have chirality. Indeed, both levorotatory (*l*-) and dextrorotatory- (*d*-) Fc-F rapidly form stable hydrogels (SI Figure S9). Interestingly, hydrogels obtained using a 1:1 mixture of *l*-Fc-F and *d*-Fc-F take significantly longer time to self-assemble than either enantiomer alone does. Figure 4C shows the circular dichroism spectra of sols generated from *d*-, *l*-, and a mixture of *d*- and *l*-Fc-F. We speculate that the chirality of the hydrogel may find application as an asymmetric synthesis catalyst support and as a gel phase in a chiral separation technique.

Super Tolerance to Salt Stress. Fc-F exhibits considerable resistance to salt stress and forms hydrogels in both saturated

NaCl solution and highly concentrated phosphate buffer. Figure 4D confirms that Fc-F retains its three-dimensional (3D) network of fibrils in saturated NaCl solution even when NaCl crystals are encapsulated in the gel, thus illustrating the robust nature of Fc-F fibrils (SI Figure S10, Fc-F fibrils encapsulate the phosphate crystals).

Additional experiments showed that Fc-F also forms stable hydrogels in concentrated transition-metal solutions (ZnCl₂, AgNO₃, CuCl₂, NiSO₄). This resistance to salt stress suggests that Fc-F hydrogels might find use as gel electrolytes. Therefore, Fc-F hydrogels might serve as a template for creating 3D networks of Zn, Co, Ni, Ag, Cu, and other metal particles by mineralization.

DISCUSSIONS

Self-assembly Step 1: From Monomers to Oligomeric

Building Blocks. Fc-F is a rare example of ferrocene derived peptides that assemble to nanofibrils. Because Fc group is a rigid and irregular moiety, the steric hindrance effect of the Fc group normally inhibits the formation of a highly packed β -sheet structure, which usually serves as the structural core of LMWP fibrils. Previous reports indicated that the Fc-LMWP-cholesterol type of organogelators assembled to spherical microparticles during gel formation.¹⁶ Insights into the interactions involved in Fc-F fibrils are of great importance to understand the formation pathway of Fc-F fibrils.

The low atomic content of Fc-F allowed us to conduct DFT calculations. The results of our DFT calculations suggest that the energetically favored conformation of an Fc-F monomer is an axe-like arrangement wherein the axe head represents the Fc moiety and the F group the handle (Figure 5A). Subsequent calculations suggest that the energetically favored conformation of an initially formed Fc-F dimer is a brick-like structure which forms via an antiparallel assembly of two monomers (Figure 5B).

It can be seen that such an antiparallel arrangement allows dual π - π stacking interactions between the Fc of each monomer and the F group of the other. This stacking configuration creates a cavity in which the carboxylic acid group of each monomer interacts with the other via a pair of hydrogen bonds; this coupling likely provides an additional driving force for dimer formation. Our DFT calculations suggest that the formation energy (ΔE) for an Fc-F dimer is 9.78 kcal·mol⁻¹.

Dimers of Fc-F can undergo oligomerization by a number of possible pathways. Here we consider two of these pathways, both involving an initial dimer-dimer interaction to form a different tetrameric species. One possible pathway results from a side-by-side interaction to form a sheet-like tetramer (Figure 5C). Inspection of the model depicted in Figure 5C shows that the side-by-side arrangement of two Fc-F dimers aligns the amido (-NH) and amido-carbonyl groups of one with a corresponding hydrogen bond acceptor or donor group of the other. We expect that this interaction would be the primary driving force for the formation of this dimer type; possible secondary stabilization might result from van der Waals interactions. DFT calculations indicate that the formation energy for this sheet-like tetramer is 24.20 kcal·mol⁻¹. The energy gap between this tetramer and two dimers is predicted to be 4.64 kcal·mol⁻¹ (24.20 - 9.78 × 2 = 4.64 kcal·mol⁻¹), suggesting the presence of interdimer forces such as hydrogen bonds and hydrophobic interactions.

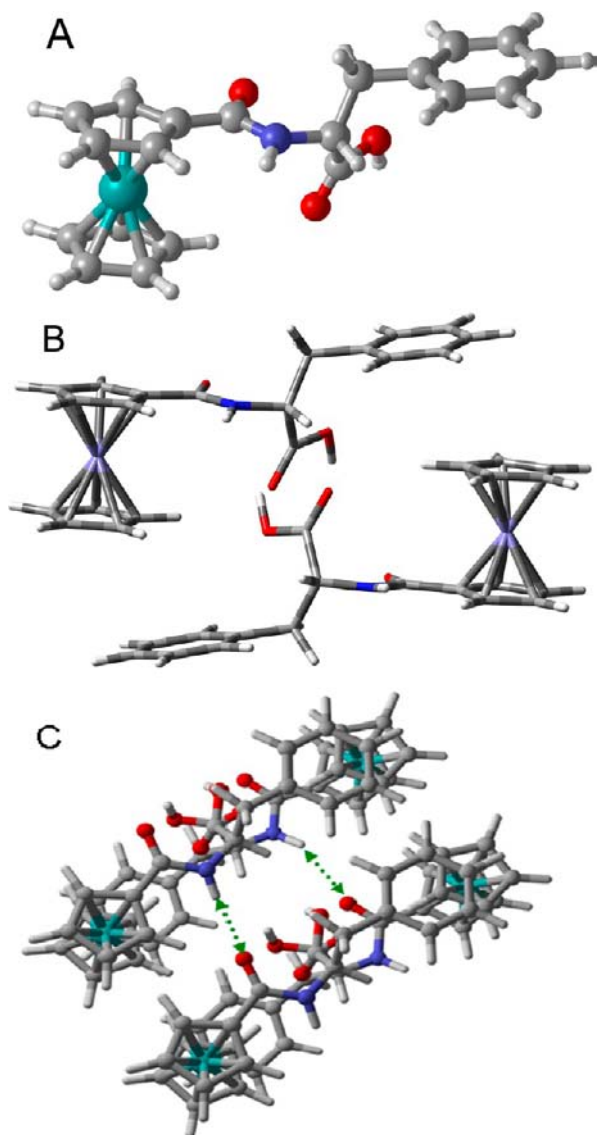


Figure 5. *Ab initio* calculation on the self-assembly pathway of the Fc-F monomer. The red bar with a white end represents an $-OH$ group, and the bar with the red end is the carbonyl group.

Self-assembly Step 2: From Oligomers to Fibrils. As noted above, another mechanism for tetramer formation would involve stacking one dimer on top of another (Figure 6). DFT

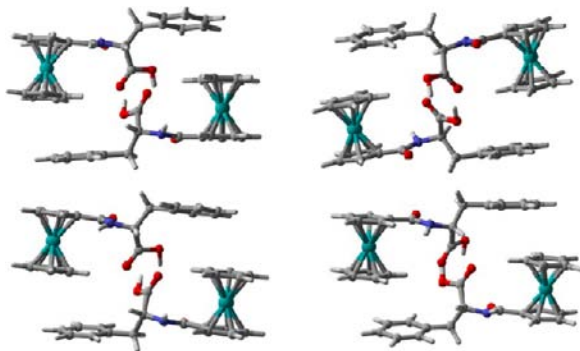


Figure 6. Two possible π - π stacking models between two nearby Fc-F dimers in two individual protofibrils, respectively.

calculations suggest in two ways that this can be accomplished, a stacked Fc-phenyl-Fc-phenyl arrangement (left model Figure 6) and a phenyl-Fc-Fc-phenyl (right model Figure 6).

Our DFT calculations predict that the ΔE for the left model is $25.30 \text{ kcal}\cdot\text{mol}^{-1}$ whereas that for the right model is $24.72 \text{ kcal}\cdot\text{mol}^{-1}$, indicating that the π - π stacking energy of two Fc-F dimers is larger than the sum of an Fc-Fc and an F-F interaction. According to the energy gap between a tetramer (left model) and two individual dimers, we can easily estimate the energy contribution of a π - π stacking interaction ($\Delta E_{\pi-\pi}$) between two stacking dimers: $\Delta E_{\pi-\pi} = \Delta E_{\text{LM}} - 2\Delta E_{\text{dimer}} = 25.30 - 9.78 \times 2 = 5.74 \text{ kcal}\cdot\text{mol}^{-1}$. For comparison, $\Delta E_{\pi-\pi}$ of two benzene rings is typically less than $3.0 \text{ kcal}\cdot\text{mol}^{-1}$.²³ It can be seen that the π - π stacking arrangement between two dimers (Fc-F-Fc-F) is similar to the that between two monomers (but using difference faces of Fc). Supposing that the electron density values of the top and bottom faces in Fc are about the same, one can also estimate that the total energy gap between the ΔE_{dimer} and the $\Delta E_{\pi-\pi}$ is about $4.04 \text{ kcal}\cdot\text{mol}^{-1}$ ($9.78 - 5.74 = 4.04 \text{ kcal}\cdot\text{mol}^{-1}$), indicating that hydrogen bonds and hydrophobic interactions provide considerable energy contribution in stabilizing a dimer.

To characterize the possible hydrogen bonds predicted by the DFT calculation, we respectively performed the Fourier transform infrared spectra (FTIR) for a series of different samples of Fc-F (presented in Figure 7).

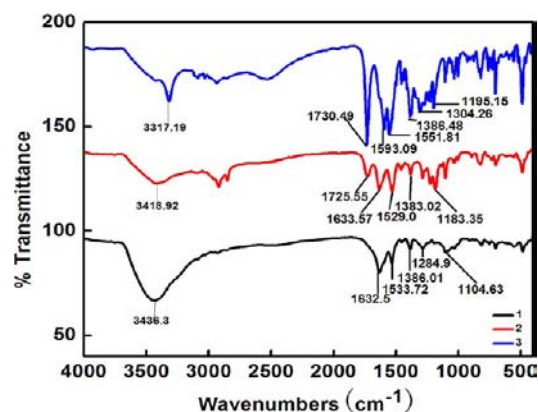


Figure 7. FTIR curves of (1) cryo-dried hydrogel, (2) HFIP treated sample, and (3) cryo-dried Fc-F power, respectively.

The IR curve of cryo-dried Fc-F hydrogel (black curve) exhibits a strong and broad adsorption peak around wavenumber 3436 cm^{-1} , corresponding to a typical hydrogen bond adsorption. The similar adsorption peak of Fc-F power (blue curve) is much weaker and sharper, referring to weak and insufficient hydrogen bond interactions in this sample. Notably, the spectrum of powdered Fc-F exhibits two relatively strong absorbance peaks at 1730 and 1593 cm^{-1} , suggesting the possibility of a carbonyl moiety and an amido moiety, respectively. The second spectrum obtained by treating a cryo-dried sample of Fc-F gel with hexafluoroisopropanol (HFIP), a well-know hydrogen bond donor, showed a new adsorption peak at 1633 cm^{-1} and a diminished carbonyl peak at 1725 cm^{-1} , which is consistent with a hydrogen bonded carbonyl group. Under the same conditions, the IR peak originally appearing at 1593 cm^{-1} , which we assign to the amido, shifted to 1529 cm^{-1} . Using these peak shifts as a precedent, we measured the IR spectrum of cryo-dried Fc-F

hydrogel and observed peaks at 1632 and 1533 cm^{-1} . These differences suggest that both the carbonyl and the amido nitrogen groups of Fc-F are involved in the formation of intermolecular hydrogen bonds during gelation.

Because oligomers have atom counts larger than those of tetramers that preclude us from performing DFT calculations, we have to develop a speculation about the mechanism of fibril formation by combining experimental observations and theoretical calculation with previous progress in this field. Two of the most successful semiempirical descriptions on the formation pathway of fibril-like structures have been formulated by Gazit et al. and Ulijin et al, respectively. Gazit's model proposes that oligomer formation results in tubular nanostructures (hollow fibrils).¹⁰ This model suggests that the basic building blocks initially assemble via a two-dimensional (2D) sheet through side-to-side π - π associations (development in the X direction) and bottom to top π - π stacking (development in the Y direction), respectively. Those 2D sheets then would curl to form hollow, tube-like structures. Ulijin's model, on the other hand, proposes that the basic building blocks periodically add to a growing oligomer to form a wire-like helix structure.¹⁹

In order to determine whether the Fc-F nanofibrils are tubular or wire-type, we compared morphological images of Fc-FF-OMe nanotubes and Fc-F fibrils (Figure 8). Nanotubes

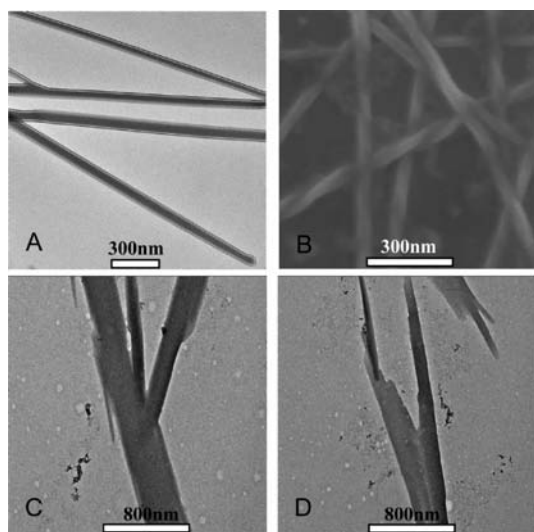


Figure 8. (A) TEM image of Fc-FF-OMe nanotubes. (B) SEM image of cryo-dried Fc-F fibrils. (C and D) TEM images of broken Fc-FF-OMe nanotubes.

typically appear to be relatively long, straight rigid structures containing occasionally tubular side branches (Figure 8A, Fc-FF-OME nanotube). Contrariwise, nanowires typically are curled and twisted and tend to be branchless (Figure 8B for SEM and SI Figure S11 for TEM). To further support for this proposal, we performed image analysis using high working voltage TEM (200 kV) on crushed Fc-FF-OME fibrils (Figure 8C and D). Inspection of these images showed the fibrils consisted of straight and branched segments that appeared to be hollow. In contrast, under similar experimental conditions, Fc-F fibrils appear to be solid (SI Figure S10).

On the basis of the above observations, we here propose a reasonable self-assembly pathway of Fc-F fibril that is different from Ulijin's closed loop cylinder (3.0 nm in diameter)¹⁹ but similar to Ulijin's proposed model of an enzyme driven

hydrogel.¹⁵ Right after the injection and incubation, Fc-F monomers first quickly assemble to dimers, and dimers may continually add onto the pre-existing aggregates by interlocking with their neighbors through side-to-side π - π stacking, perhaps also including the intermolecular hydrogen bonds. Since these Fc-F dimers are not perfect rectangles, there appears a slight angle of obliquity when dimers associate with their neighbors. Hence, Fc-F dimers may assemble in a helix fashion, leading to fibrils that contain spiral grooves. This may explain why Fc-F fibrils are much larger (at least 30 nm in diameter) and longer (1 mm or longer) compared to Fmoc-FF fibrils.

Self-assembly Step 3: From Fibrils to Hydrogels. It needs to be pointed out that the emergence of nanofibers and even networks of nanofibers do not necessarily trigger off gelation in bulk solution. Our experimental results revealed that the Fc-F sols, and its methanol and ethanol solution also contained 2D networks of fibrils, but exhibited no gels (SI Figures S12 and S13).

To find out that if this exists a conformation transition of Fc-F fibril during the gelation process, we recorded ultraviolet (UV) and circular dichroism (CD) signal changes with the increase of concentration of Fc-F shown in Figure 9A and B, respectively.

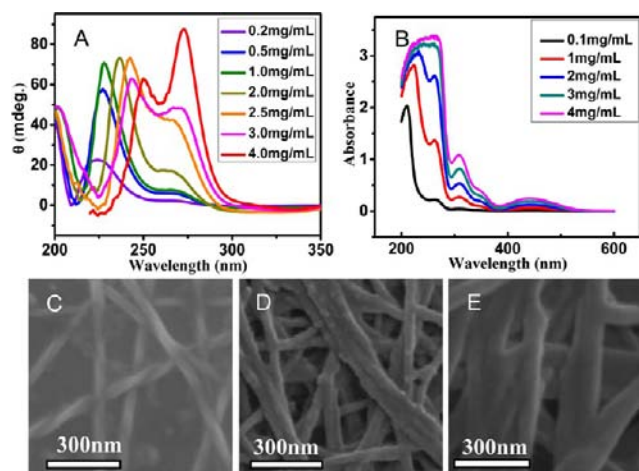


Figure 9. (A, B) UV and CD spectra of Fc-F gel at different concentrations. (C–E) SEM images of cryo-dried Fc-F gel at 2 $\text{mg}\cdot\text{mL}^{-1}$, 3 $\text{mg}\cdot\text{mL}^{-1}$, and 5 $\text{mg}\cdot\text{mL}^{-1}$, respectively.

Our CD curves exhibit two major adsorption peaks at 230 and 270 nm, respectively. The intensity of the first peak increased with the increase of Fc-F concentration below 2.5 $\text{mg}\cdot\text{mL}^{-1}$. Above this concentration value, the intensity of the first peak changed little. The second peak grew slowly till the bulk concentration reached 2.0 $\text{mg}\cdot\text{mL}^{-1}$. Above this concentration, the intensity of this peak increased significantly. Notably, the maximum adsorption position of both peaks continually red-shifts as the concentration increases over the entire concentration range.

The UV spectra have four adsorption peaks at around 230, 270, 330, and 450 nm, respectively. The main peak (230 nm) also exhibited a significant red-shift according to the concentration increase. To our knowledge, one possible process that may lead to the optical signal red-shift is the so-called H aggregate (face to face arrangement, building blocks align parallel to each other but perpendicular to the line joining their centers) to J aggregate (end to end arrangement, building block

aligns parallel to the center line) conformational transition of the aggregates.²⁴

Yao *et al.* observed a significant blue to red color variation on the fibrils of their dye according to the concentration increasing (from 1 to 5 mM) by polarized-light microscopy. They reported that the nanofibrous structures of those dyes changed a little at the same time.²⁴ They suggested that this phenomenon was caused by the conformation transition of their nanofibrils, from the H aggregate state to the J aggregate state.

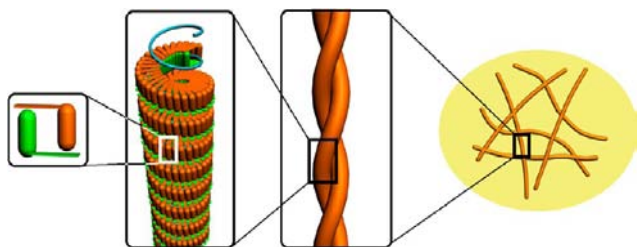
It is difficult for us to comprehend that, in our case, aggregation state changes of the basic build blocks (for instance, dimers in fibrils taking an H to J change) are still energy favored processes after the formation of Fc-F fibrils. Therefore, we carefully reviewed the images of Yao *et al.* and noticed the coexistence of thin blue fibrils with the thicker red fibrils in their samples. This observation reminds us that there may be another possible explanation for the signal red-shift phenomenon in our experiments. We here regard the individual fibril as the initial building blocks, and the concentration increase of the Fc-F favors the formation of intertwined fibrils or ribbons in bulk solution. Supposing that, the assembly of protofibrils to the matured fibrils or ribbons is in a J-aggregate mode, the optical signals of matured fibril will exhibit red-shifted all the same. In other words, the formation of a twisted-pair by two individual protofibrils itself may also lead to the overall signals red-shift, regardless of the absolute conformation (J or H mode) of initial building units (in this case, proto-fibrils).

We synchronously monitored the morphological changes of those fibular aggregates in Fc-F sol and highly concentrated gel system, respectively. Figure 9C, D, and E show SEM images of cryo-dried Fc-F sol ($2 \text{ mg}\cdot\text{mL}^{-1}$), Fc-F gel ($3 \text{ mg}\cdot\text{mL}^{-1}$), and Fc-F gel ($5 \text{ mg}\cdot\text{mL}^{-1}$), respectively, revealing that the red-shift of the UV and CD signals accompanies the widening of fibril diameters. Therefore, we believe that the red-shift of the optical signals may be caused by the postfibrillar assembly of ribbons or twist ropes, corresponding to an apparent H to J change.

In order to gain greater details regarding the morphological structure of Fc-F hydrogels, we studied gel fibrils with the aid of confocal Raman microscopy (SI Figure S14). Analyses of the images generated in this way show these matured fibrils are several millimeters in length and $2\text{--}20 \mu\text{m}$ in diameter, suggesting that they are fabricated from thinner and shorter protofibrils.

Combining structural analysis with optical and electrical measurements, we here propose a stepwise hierarchical assembly in the fibril formation, shown in Scheme 1, which formulates a possible pathway for the formation of Fc-F hydrogels. Initial stages of this process, as described above, involve dimer and tetramer formation that are energized by a

Scheme 1. Schematic Illustration of a Possible Formation Pathway of a Fc-F Hydrogel



variety of $\pi\text{--}\pi$ and hydrogen bonds. Tetramers assemble to afford a protofibril, and two protofibrils twist to a matured fibril. Matured fibrils may directly undergo cross-linking, which results in 3D networks, or further associate into ribbon-like structures that form cross-linked 3D networks. Ferrocenyl groups are critical to Fc-F fibril formation, which is reflected by the fact that oxidatively changing the aromatic state of the Fc moiety can significantly affect the self-assembly behavior of Fc-F or the stability of its hydrogels.

Our model may explain why strong shearing stress (such as shaking) induces a gel to sol transformation, whereas gentle stirring promotes the reverse process. We have shown that Fc-F fibrils are strong enough to survive a drying process in the presence of high concentrations of salt, which suggests that Fc-F fibrils can tolerate stretching forces along its long-axis. However, our SEM images suggest that the shaking-induced suspensions contained many short fibrils and large ribbons (SI Figure S15). Our explanation for this observation is that a strong shear force such as heavy shaking may only break the connections among the cross-linked matured fibrils and therefore induce the gel-to-sol transition; gentle stirring helps re-establish interfibrils association, thereby restoring the hydrogel.

CONCLUSION

In summary, we have demonstrated that ferrocenyl phenylalanine, Fc-F, is a multistimuli responsive hydrogelator that reversibly and rapidly responds to changes in redox potential, pH, temperature, and agitation. Fc-F is characterized by an exceptionally simple molecular structure and, to the best of our knowledge, is the most compact stimuli responsive hydrogelator that has ever been reported. In addition, its design constitutes a remarkably facile method for introducing an electrochemically active organometallic moiety into a gel. We performed DFT calculations that predict the energies and possible geometries of monomeric, dimeric, and tetrameric arrangements that Fc-F might experience during the self-assembly process that may lead to gelation. On the basis of observations gathered using a variety of microscopic imaging techniques, we have proposed a tentative mechanism of oligomerization. A key component of this hypothesis is that the complementary $\pi\text{--}\pi$ and hydrogen bonding takes place between the ferrocenyl and benzene rings of the phenylalanine moieties and between both carboxylic acid groups, respectively, during dimer formation. Of equal importance is the hydrogen bond promoted assembly of two dimers in a side by side fashion to generate tetramers and $\pi\text{--}\pi$ bonding to form a stacked tetrameric species. The excellent stability and extremely high salt tolerance of Fc-F gel suggests it might find use as a controllable drug medium or as a chiral catalyst. We expect that Fc-F will serve as a valuable archetypical template for future researchers who will use when designing new, multiresponsive hydrogelators. Work to extend the concepts discussed in this report, especially the use of metallic dicyclopentadienyl ring systems in place of ferrocene, is currently in progress.

ASSOCIATED CONTENT

Supporting Information

Experimental procedures and characterization data. This material is available free of charge via the Internet at <http://pubs.acs.org>.

■ AUTHOR INFORMATION

Corresponding Author

yzhangcsu@csu.edu.cn

Author Contributions

^{||}Z.S. and Z.L. contributed equally to this work.

Notes

The authors declare no competing financial interest.

■ ACKNOWLEDGMENTS

This work was supported by the National Natural Science Foundation of China (91127024, 20973201, 21105128, and 21275164) and the Natural Science Foundation of Hun Nan Province (11JJ3017). The authors acknowledge James Foley for constructive advice and editorial assistance. We thank Prof. Helmuth Möhwald, Dianlu Jiang, Juan Xiang, Younian Liu, and Jianxiu Wang for valuable discussions and for their help with DFT calculations. We are grateful for technical support from the High Performance Computing Center of Central South University.

■ REFERENCES

- (1) Terech, P.; Weiss, R. G. *Chem. Rev.* **1997**, *97*, 3133–3160. Piepenbrock, M. O. M.; Lloyd, G. O.; Clarke, N.; Steed, J. W. *Chem. Rev.* **2009**, *110*, 1960–2004. Sangeetha, N. M.; Maitra, U. *Chem. Soc. Rev.* **2005**, *34*, 821–836. Segarra-Maset, M. D.; Nebot, V. J.; Miravet, J. F.; Escuder, B. *Chem. Soc. Rev.* **2012**, DOI: 10.1039/C2CS35436E.
- (2) Feringa, B. L. J. *Org. Chem.* **2007**, *72*, 6635–6652.
- (3) Seo, Y. J.; Bhuniya, S.; Kim, B. H. *Chem. Commun.* **2007**, *18*, 1804–1806. Teng, M. J.; Kuang, G. C.; Jia, X. R.; Gao, M.; Li, Y.; Wei, Y. J. *Mater. Chem.* **2009**, *19*, 5648–5654. Wadhavane, P. D.; Izquierdo, M. A.; Galindo, F.; Burguete, M. I.; Luis, S. V. *Soft Matter* **2012**, *8*, 4373–4381.
- (4) Yan, X.; Xu, D.; Chi, X.; Chen, J.; Dong, S.; Ding, X.; Yu, Y.; Huang, F. *Adv. Mater.* **2012**, *24*, 362–369.
- (5) Gao, Y.; Kuang, Y.; Guo, Z. F.; Guo, Z. H.; Krauss, I. J.; Xu, B. J. *Am. Chem. Soc.* **2009**, *131*, 13576–13577. Koutsopoulos, S.; Unsworth, L. D.; Nagai, Y.; Zhang, S. *Proc. Natl. Acad. Sci.* **2009**, *106*, 4623–4628. Zhao, F.; Ma, M. L.; Xu, B. *Chem. Soc. Rev.* **2009**, *38*, 883–891. Li, X.; Li, J.; Gao, Y.; Kuang, Y.; Shi, J.; Xu, B. *J. Am. Chem. Soc.* **2010**, *132*, 17707–17709. Boekhoven, J.; Koot, M.; Wezendonk, T. A.; Eelkema, R.; van Esch, J. H. *J. Am. Chem. Soc.* **2012**, *134*, 12908–12911. Naskar, J.; Palui, G.; Banerjee, A. *J. Phys. Chem. B* **2009**, *113*, 11787–11792.
- (6) Kimizuka, N.; Nakashima, T. *Langmuir* **2001**, *17*, 6759–6761. Kubo, W.; Kambe, S.; Nakade, S.; Kitamura, T.; Hanabusa, K.; Wada, Y.; Yanagida, S. *J. Phys. Chem. B* **2003**, *107*, 4374–4381. Krieg, E.; Shirman, E.; Weissman, H.; Shimon, E.; Wolf, S. G.; Pinkas, I.; Rybtchinski, B. *J. Am. Chem. Soc.* **2009**, *131*, 14365–14373.
- (7) Ajayaghosh, A.; Praveen, V. K. *Acc. Chem. Res.* **2007**, *40*, 644–656. Kato, T.; Hirai, Y.; Nakaso, S.; Moriyama, M. *Chem. Soc. Rev.* **2007**, *36*, 1857–67. Carretti, E.; Bonini, M.; Dei, L.; Berrie, B. H.; Angelova, L. V.; Baglioni, P.; Weiss, R. G. *Acc. Chem. Res.* **2010**, *43*, 751–760. Foster, J. A.; Steed, J. W. *Angew. Chem., Int. Ed.* **2010**, *49*, 6718–6724. Jung, J. H.; Park, M.; Shinkai, S. *Chem. Soc. Rev.* **2010**, *39*, 4286–302. Le Bideau, J.; Viau, L.; Vioux, A. *Chem. Soc. Rev.* **2011**, *40*, 907–25. Das, D.; Kar, T.; Das, P. K. *Soft Matter* **2012**, *8*, 2348–2365.
- (8) Wang, C.; Zhang, D.; Zhu, D. *J. Am. Chem. Soc.* **2005**, *127*, 16372–16373. Wang, C.; Chen, Q.; Sun, F.; Zhang, D.; Zhang, G.; Huang, Y.; Zhao, R.; Zhu, D. *J. Am. Chem. Soc.* **2010**, *132*, 3092–3096. Dastidar, P. *Chem. Soc. Rev.* **2008**, *37*, 2699–715. Roy, S.; Banerjee, A. *Soft Matter* **2011**, *7*, 5300–5308. Tomasini, C.; Castellucci, N. *Chem. Soc. Rev.* **2012**, *42*, 156–172. Peng, F.; Li, G.; Liu, X.; Wu, S.; Tong, Z. *J. Am. Chem. Soc.* **2008**, *130*, 16166–16167. Tomasini, C.; Castellucci, N. *Chem. Soc. Rev.* **2013**, *42*, 156–172. Ou, C. W.; Zhang, J. W.; Zhang, X. L.; Yang, Z. M.; Chen, M. S. *Chem. Commun.* **2013**, *49*, 1853–1855. Zheng, W. T.; Gao, J.; Song, L. J.; Chen, C. Y.; Guan, D.;

Wang, Z. H.; Li, Z. B.; Kong, D. L.; Yang, Z. M. *J. Am. Chem. Soc.* **2013**, *135*, 266–271. Celis, S.; Nolis, P.; Illa, O.; Branchadell, V.; Ortono, R. M. *Org. Biomol. Chem.* **2013**, *11*, 2839–2846. Komatsu, H.; Matsumoto, S.; Tamaru, S. i.; Kaneko, K.; Ikeda, M.; Hamachi, I. *J. Am. Chem. Soc.* **2009**, *131*, 5580–5585.

(9) Eitouni, H. B.; Balsara, N. P. *J. Am. Chem. Soc.* **2004**, *126*, 7446–7447. Medina, J. C.; Gay, I.; Chen, Z.; Echegoyen, L.; Gokel, G. W. *J. Am. Chem. Soc.* **1991**, *113*, 365–366. Nakahata, M.; Takashima, Y.; Yamaguchi, H.; Harada, A. *Nat. Commun.* **2011**, *2*, 1–6. Tan, L.; Liu, Y.; Ha, W.; Ding, L. S.; Peng, S. L.; Zhang, S.; Li, B. *J. Soft Matter* **2012**, *8*, 5746–5749.

(10) Mahler, A.; Reches, M.; Rechter, M.; Cohen, S.; Gazit, E. *Adv. Mater.* **2006**, *18*, 1365–1370. Gazit, E. *FASEB J.* **2002**, *16*, 77–83. Reches, M.; Gazit, E. *Science* **2003**, *300*, 625–627.

(11) Yan, N.; Xu, Z.; Diehn, K. K.; Raghavan, S. R.; Fang, Y.; Weiss, R. G. *J. Am. Chem. Soc.* **2013**, *135*, 8989–8999. Zheng, W.; Gao, J.; Song, L.; Chen, C.; Guan, D.; Wang, Z.; Li, Z.; Kong, D.; Yang, Z. *J. Am. Chem. Soc.* **2013**, *135*, 266–271.

(12) Su, Y.; Yan, X.; Wang, A.; Fei, J.; Cui, Y.; He, Q.; Li, J. *J. Mater. Chem.* **2010**, *20*, 6734–6740. Yan, X.; Cui, Y.; He, Q.; Wang, K.; Li, J. *Chem. Mater.* **2008**, *20*, 1522–1526. Yan, X.; Zhu, P.; Li, J. *Chem. Soc. Rev.* **2010**, *39*, 1877–1890. Zhu, P.; Yan, X.; Su, Y.; Yang, Y.; Li, J. *Chem.—Eur. J.* **2010**, *16*, 3176–3183. Du, M.; Song, W.; Cui, Y.; Yang, Y.; Li, J. *J. Mater. Chem.* **2011**, *21*, 2228–2236.

(13) Ulijn, R. V.; Smith, A. M. *Chem. Soc. Rev.* **2008**, *37*, 664–675.

(14) Gao, Y.; Shi, J.; Yuan, D.; Xu, B. *Nat. Commun.* **2012**, *3*, 1033. Gao, Y.; Zhao, F.; Wang, Q.; Zhang, Y.; Xu, B. *Chem. Soc. Rev.* **2010**, *39*, 3425–3433. Li, J.; Kuang, Y.; Gao, Y.; Du, X.; Shi, J.; Xu, B. *J. Am. Chem. Soc.* **2012**, *135*, 542. Ma, M. L.; Kuang, Y.; Gao, Y.; Zhang, Y.; Gao, P.; Xu, B. *J. Am. Chem. Soc.* **2010**, *132*, 2719–2728. Yang, Z.; Liang, G.; Ma, M.; Gao, Y.; Xu, B. *J. Mater. Chem.* **2007**, *17*, 850–854. Zhang, Y.; Gu, H.; Yang, Z.; Xu, B. *J. Am. Chem. Soc.* **2003**, *125*, 13680–13681. Adhikari, B.; Banerjee, A. *Soft Matter* **2011**, *7*, 9259–9266. De Groot, N. S.; Parella, T.; Aviles, F. X.; Vendrell, J.; Ventura, S. *Biophys. J.* **2007**, *92*, 1732–1741. Chen, J.; McNeil, A. J. *J. Am. Chem. Soc.* **2008**, *130*, 16496–16497.

(15) Hirst, A. R.; Roy, S.; Arora, M.; Das, A. K.; Hodson, N.; Murray, P.; Marshall, S.; Javid, N.; Sefcik, J.; Boekhoven, J.; van Esch, J. H.; Santabarbara, S.; Hunt, N. T.; Ulijn, R. V. *Nat. Chem.* **2010**, *2*, 1089–1094.

(16) Liu, J.; He, P.; Yan, J.; Fang, X.; Peng, J.; Liu, K.; Fang, Y. *Adv. Mater.* **2008**, *20*, 2508–2511.

(17) Krieg, R.; Wyrwa, R.; Mollmann, U.; Gorus, H.; Schonecker, B. *Steroids* **1998**, *63*, 531–541. Weber, B.; Serafin, A.; Michie, J.; Van Rensburg, C.; Swarts, J. C.; Bohm, L. *Anticancer Res.* **2004**, *24*, 763–770.

(18) Degani, Y.; Heller, A. *J. Phys. Chem.* **1987**, *91*, 1285–1289.

(19) Smith, A. M.; Williams, R. J.; Tang, C.; Coppo, P.; Collins, R. F.; Turner, M. L.; Saiani, A.; Ulijn, R. V. *Adv. Mater.* **2008**, *20*, 37–41.

(20) Goodwin, J. W.; Hughes, R. W. *Rheology for Chemistry: An introduction*; Royal Society of Chemistry: Cambridge, 2000.

(21) Abasq, M. L.; Saidi, M.; Burgot, J. L.; Darchen, A. *J. Org. Chem.* **2009**, *694*, 36–42.

(22) Sun, Z.; Deng, L.; Gan, H.; Shen, R.; Yang, M.; Zhang, Y. *Biosens. Bioelectron.* **2013**, *39*, 215–219.

(23) Grimme, S. *J. Comput. Chem.* **2004**, *25*, 1463–1473. Jurecka, P.; Cerny, J.; Hobza, P.; Salahub, D. R. *J. Comput. Chem.* **2007**, *28*, 555–569. Waller, M. P.; Robertazzi, A.; Platts, J. A.; Hibbs, D. E.; Williams, P. A. *J. Comput. Chem.* **2006**, *27*, 491–504. Johnson, E. R.; Keinan, S.; Mori-Sanchez, P.; Contreras-Garcia, J.; Cohen, A. J.; Yang, W. *J. Am. Chem. Soc.* **2010**, *132*, 6498–6506.

(24) Yao, H.; Domoto, K.; Isohashi, T.; Kimura, K. *Langmuir* **2005**, *21*, 1067–1073.